Supporting information

Energy recovery from concentrated seawater brine by thin-film nanofiber composite pressure retarded osmosis membranes with high power density

Xiaoxiao Song, and *Zhaoyang Liu** and *Darren Delai Sun* *

School of Civil and Environmental Engineering, Nanyang Technological University, 639798 (Singapore)

*Please address correspondence to either author. Z.Y.Liu: E-mail: zyliu@ntu.edu.sg; Tel: +65 8298 7689; Fax: +65 6791 0676. D.D.Sun: E-mail ddsun@ntu.edu.sg); Tel: +65 67906273; Fax: +65 6791 0676.

The supporting information includes 16 pages (S1-S17) and 8 images (Figure S1-S8).

Determination of membrane intrinsic parameters and salt rejection

Pure water permeability (A) is determined by a bench scale cross-flow RO unit (SEPA CF II, GE, 140 cm^2 effective area).[1] Spacers (sterlitech, Sepa CF feed spacer, 17 mil) were inserted. The cross-flow was maintained at 15.4 cm s^{-1}. The loaded membrane was subject to pure water compaction at 10 Bar for at least 3 h. Then the pressure was lowered to a series of values (ΔP) and the corresponding water flux J_W was measured. The A can be obtained by dividing J_W with ΔP (J_W=A* ΔP).[2]

The salt permeability (B) and structure parameter (S) was determined based on water flux, J_W, and solute flux, J_S, in FO configuration. 0.5 M NaCl and DI water was employed as draw solution and feed solution respectively. A custom-built rectangular acrylic plastic FO module nailed by 6 screws (3 on long side and 2 on short side). Two rubber O-rings are used to seal the channels. The depths of channels on the feed and draw solutions side are 2mm. The module has an effective membrane area of 23.8 cm^2. Cross-flow velocities at both feed solution and draw solution sides were maintained by gear pump (cole-palmer) at 16.7 cm s^{-1}. Spacers (Sepa CF feed spacer, 17 mil) were set in the 2 mm deep channels on both sides inside. While equilibrium was reached, the conductivity and weight change of feed and draw solutions were monitored with 2 minutes intervals. The $C_{F,b}$ and J_W can be derived from the monitored data.[1] According to mass balance equation:

$$C_{F,b}(V_0 - J_W * A_m * t) = C_{F,b0} * V_0 + J_S * A_m * t \quad \text{(S1)}$$

Wherein $C_{F,b}$ is the bulk feed solute concentration at time *t*. V_0 is the original feed solution volume. J_W is the measured water flux, A_m is the membrane area and $C_{F,b0}$ is the original bulk feed solute concentration. J_s is the solute flux, which is rewritten as:[3]

$$J_S = B * C_{D,b} * \exp(-J_W S / D) \quad \text{(S2)}$$

Wherein $C_{D,b}$ is the bulk draw solute (NaCl) concentration, D is the solute diffusion coefficient.[4] S, the membrane structure parameter, can be calculated from.[5]

$$S = \left(\frac{D}{J_W}\right) * \ln((B + A * \pi_{D,b})/(B + J_W)) \quad \text{(S3)}$$

Wherein $\pi_{D,b}$ is the osmotic pressure of bulk draw solute (NaCl). The above equation S1, S2 and S3 have three unknown variables, thus J_S, B and S can be solved.

The test conditions for determination of salt rejection, R, were as follows: Feed solution=50mM NaCl. Applied pressure=15 Bar. Cross Flow Velocity=15.4 cm/S. The Sterlitech high foulant feed spacer and permeate carrier spacer were inserted on the feed solution side and permeate solution side, respectively. Test temperature was at 25 °C. Then concentrated NaCl solution (2 M) was added to the feed tank to adjust total feed concentration to be 50 mM. When the permeate water flux became stabilized, the samples were collected from permeate outlet and concentrate outlet collected and determined using conductivity meter. The concentration thus calculated was used as C_p and C_f respectively. The rejection, R, can be calculated by the equation $(1-C_p/C_f)$ in a typical RO process.

Determination of PRO water flux

The schematic diagram of the PRO system is shown in Figure S2. The stainless-steel membrane module, which was a modified version of a commercial cross flow cell (GE SEPA II, Osmonics) has an effective area of 140 cm^2.[22] The unit was working with spacers (sterlitech feed spacers, diamond) inserted within the 2mm deep flow channel on both draw and feed solution sides. The flow scheme was counter-current. The feed solution was circulated at a flow rate of 0.8 L min^{-1} with a variable-speed gear pump (Cole Parmer). The draw solution was pressurized with a high pressure pump (Hydra-cell pump) and circulated at a flow rate of 0.8 L min^{-1}. The frequency of the pump and a valve at the outlet of the membrane module controls the hydraulic pressure and cross flow velocity respectively. A customized water bath was use to control the temperature of both feed and draw solutions constantly at 25±1°C.

The PRO experiment was conduct with 4 liters synthetic seawater brine (SB) as draw solution and 1 liter brackish water (BW) or river water (RW) feed solution, respectively. The TNC-PRO membranes were placed in the membrane module with selective layer facing draw solution. To ensure the membrane is conditioned to the maximum pressure, we pre-run the membrane with 15.2 Bar with pure water, then concentrated draw solution were added into the draw solution circuit to adjust the overall draw solution concentration to be 1.06 M. After the temperature and the flux became stabilized, the weight of the digital balance is recorded every 2 minutes. And the averaged J_W is calculated based on 5 data points every 10 minutes. The ΔP is reduced to 13.3, 10.2, 8.8, 7.5, 5.8, 4.9, 3.8, 2.5 and 0 Bar stepwise and the respective

J_W is recorded. Thus, for each of the TNC-PRO membranes, the series of J_W has 10 data points, corresponding to the above ΔP.

Significance of performance limiting factors for TNC-2 membrane (BW-SB)

While accounting for ECP, ICP, and RSP, the modeling of Equation 3 and 4 suggests that ΔC_m is substantially lower than the nominal solute concentration difference between the feed and draw solutions. The reduction of ΔC_m then translates into loss of J_W and W. For all TNC-PRO membranes, the experimental J_W fits well with the projected J_W using this model (upper plot in Figure 3 in main text). The successful prediction of J_W by this model for phase-inversion PRO membranes and commercial PRO membranes were also reported in a previous study.[43] In Figure S5, the realistic W curve, W_{real}, and ideal W curve, W_{ideal}, for TNC-2 membrane working in BW-SB configuration is represented by black curve and grey dotted curve, respectively. By assuming the elimination of the RSP (B/J_W*[exp($J_W S/D$)-exp(-J_W/k)]=0), ICP (exp($J_W S/D$)-1=0) or ECP (1-exp(-J_W/k)=0), the W loss to each limiting phenomenon is restored. The resulted hypothesized $W_{no\text{-}RSP}$, $W_{no\text{-}RSP}$ and $W_{no\text{-}RSP}$ curve is represented by the dashed green, red and blue curve respectively. The significance of each limiting phenomenon can be evaluated by comparing the according curve with W_{real}. The bigger difference it shows, the more significant is the limiting effect of the according phenomenon. In this sense, the significance of the limiting phenomenon follow the order of ECP>ICP>RSP, as shown in Figure S5. To quantify the significance of each limiting phenomenon, the projected peak power density (W_p) at

the top of the projected W curves are used as the benchmark value. The TNC-2 membrane is predicted to output the highest $W_{p,real}$ of 15.2 W m^{-2} at a ΔP of 22.6 Bar. Due to a synergistic limiting effect by ECP, ICP and RSP, this value is still far less than the ideal value, $W_{p,ideal}$. However, when the limiting effect of ECP, ICP or RSP is eliminated, the W_p is restored to $W_{p,no\text{-}ECP}$, $W_{p,no\text{-}ICP}$ and $W_{p,no\text{-}RSP}$ respectively.

Derivation of Equation 5 (variable-ΔP model) for total energy recovery from seawater brine

We assume that the rejection of the membrane for NaCl is 100% and no reverse salt permeation (RSP) happened. Thus by the law of mass conservation equation, the mass of NaCl in the draw solution will not change. Now, the initial concentration and volume of brine is C_0 (C_0=1.06 M) and V_0 respectively. We introduce a ϕ value to represent the fraction of initial volume of feed solution over the initial volumes of both feed and draw solutions. Thus the initial volume of feed solution can be expressed as: $[\phi/(1-\phi)]*V_0$. In a variable-ΔP model, the ΔP is continuously decreased. The process will only stop when initial volume of feed solution, $[\phi/(1-\phi)]*V_0$, completely permeate through the membrane. At the terminal status, the draw solution will be diluted to $(1-\phi)* C_0$.

At an intermediate time t, the C_0 is diluted to C_t and the volume of the brine increases to V_t. After an infinitesimal period of time, dt, the concentration and volume is C_{t+dt} and V_{t+dt} respectively. We have:

$$C_0 * V_0 = C_t * V_t = C_{t+dt} * V_{t+dt} \quad \text{(S4)}$$

In the above equation the C_t and V_t fulfills the continuity of functions:

$$C_{t+dt} = (C_t + dC) \text{ and } V_{t+dt} = (V_t + dV) \quad \text{(S5)}$$

Furthermore, the dV can be re-written as:

$$dV = J_W * A_m * dt \quad \text{(S6)}$$

In which J_W is the trans-membrane water flux at time t, A_m is the effective area in operation. Combining equation (1-3) concludes:

$$C_t * V_t = (C_t + dC) * (V_t + J_W * A_m * dt) \quad \text{(S7)}$$

Rearranging equation (4) and ignore the second order infinitesimal term ($J_W * A_m * dt * dC$) on the right, we have:

$$V_t * dC + C_t * J_W * A_m * dt = 0 \quad \text{(S8)}$$

Substituting equation (1) into equation (4), we have:

$$(\frac{C_0 V_0}{C_t}) * dC + C_t * J_W * A_m * dt = 0 \quad \text{(S9)}$$

Note that:

$$J_W * A_m * dt = dE / \Delta P \quad \text{(S10)}$$

Combining equation (6) and (7) we conclude the calculation of dE as a function of C_0 and ΔP:

$$dE = -C_0 V_0 * \frac{1}{C_t^2} * \Delta P * dC \quad \text{(S11)}$$

Integrating equation S11 from C_0 (initial $C_{D,b}$) to (1- ϕ)* C_0 (final $C_{D,b}$) we have:

$$E = -C_0 * \int_{C_0}^{(1-\phi)*C_0} (\Delta P / C_t^2) * dC \quad \text{(S12)}$$

Constant-ΔP model for the calculation of energy recovery rate

Following the model developed in a recent study (Yip and Elimelech, ES&T, 2012 (46), 5230–5239), the practical extractable work can be expressed as:

$$W_{p,\max} = \nu RT(1-\phi)(\sqrt{C_D^0} - \sqrt{C_F^0})^2 V_F^0 \quad \text{(S13)}$$

$$\phi \approx V_F^0 / (V_F^0 + V_D^0) \quad \text{(S14)}$$

Wherein, V_F^0 is the initial volume of feed solution and V_D^0 is the initial volume of draw solution. This $W_{p,max}$ stands for the maximum extractable work at a constant ΔP for given volumes of feed solution and draw solution without considering the PRO membrane properties. In the above equation, the value of $W_{p,max}/V_F^0$ suggests the energy production per unit volume of feed solution.

In our study, the energy recovery rate is defined by energy production per unit volume of draw solution (i.e. seawater brine). To make the calculation comparable with the value in our study, we use a different form of the above equations by substituting equation S14 into equation S13:

$$W_{p,\max} = \Delta P * \Delta V^* = \nu RT\phi(\sqrt{C_D^0} - \sqrt{C_F^0})^2 V_D^0 \quad \text{(S15)}$$

In this equation, the $W_{p,max}/V_D^0$ is the energy production per unit volume of draw solution (seawater brine). Thus the physical meaning can be unified with its equivalent in the variable-ΔP model.

In the previous publication (Yip and Elimelech, ES&T, 2012 (46), 5230–5239), the parameter ϕ was assigned a value of ϕ=0.4. However in our revised manuscript we assign a value of 0.75, this is because the concentration of seawater brine (considering system recovery of 50%) is about 2 times of the concentration of seawater. It should be noted here that in the variable-ΔP model, the value of ϕ=0.75 was also adopted.

Calculation of Gibbs free mixing energy, ΔG_{mix}

The ΔG_{mix} is calculated based on a previous literature (Yip and Elimelech, ES&T, 2012 (46), 5230–5239, Equation 5) in a modified form considering that ($V_A/V_B \approx \phi/(1-\phi)$):

$$-\frac{\Delta G_{mix,V_B}}{\nu RT} \approx \left(\frac{c_M}{\phi}\ln c_M - c_A \ln c_A - \frac{1-\phi}{\phi} c_B \ln c_B\right) * \left(\frac{\phi}{1-\phi}\right) \quad \text{(S16)}$$

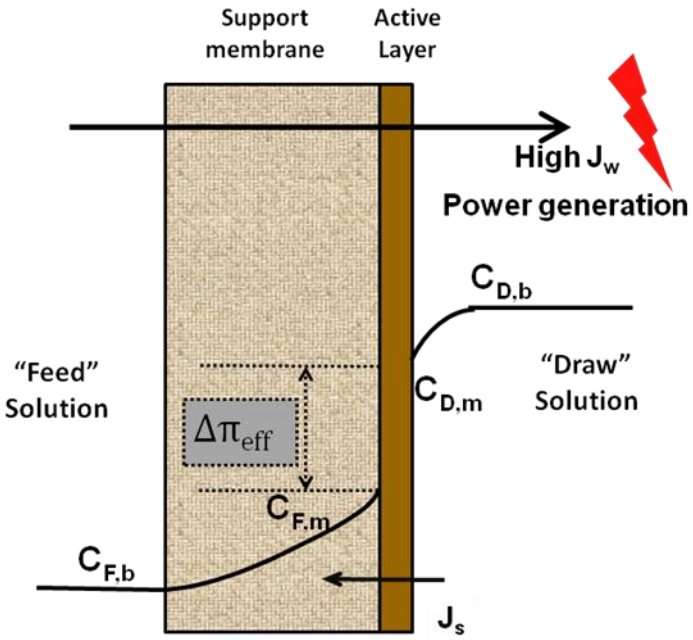

Figure S1. The schematic drawing of working principle of PRO membrane. Water flows naturally from low salinity feed solution ($C_{F,b}$) to high salinity draw solution ($C_{D,b}$). The water flux (J_w) drives a turbine, which is mounted at draw solution side, to generate power. The ICP phenomenon causes solutes to accumulate within in support membrane, resulting in increased $C_{F,m}$ at the membrane active layer. The ECP phenomenon causes solutes to be diluted at draw solution side, resulting in decreased $C_{F,m}$ at the membrane active layer. As a result, the net osmotic pressure difference ($\Delta\pi_{eff}$) across the active layer is decreased.

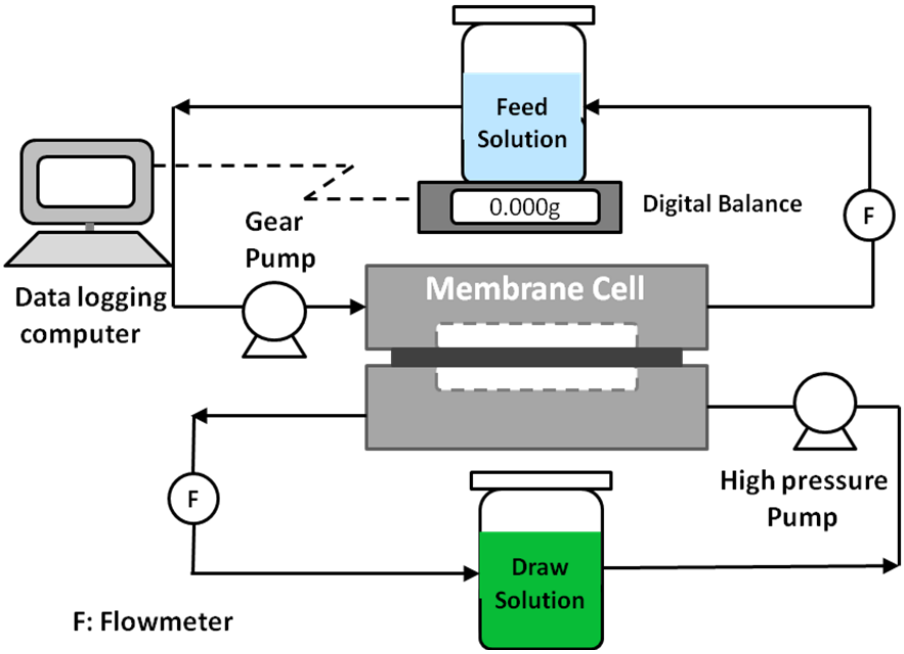

Figure S2. A schematic simplified diagram of lab-scale PRO system. The flow scheme of the draw solution and feed solution is counter-current in the membrane cell. The membrane cell is a modified stainless steel cross flow cell (GE SEPA II, Osmonics, effect area=140 cm^2). The feed solution and draw solution tanks are equipped with a cooling system (not drawn in this diagram) to constantly maintain the temperature at 25 ± 1°C. A data logging balance measures the weight change of the feed solution, from which the J_W is calculated.

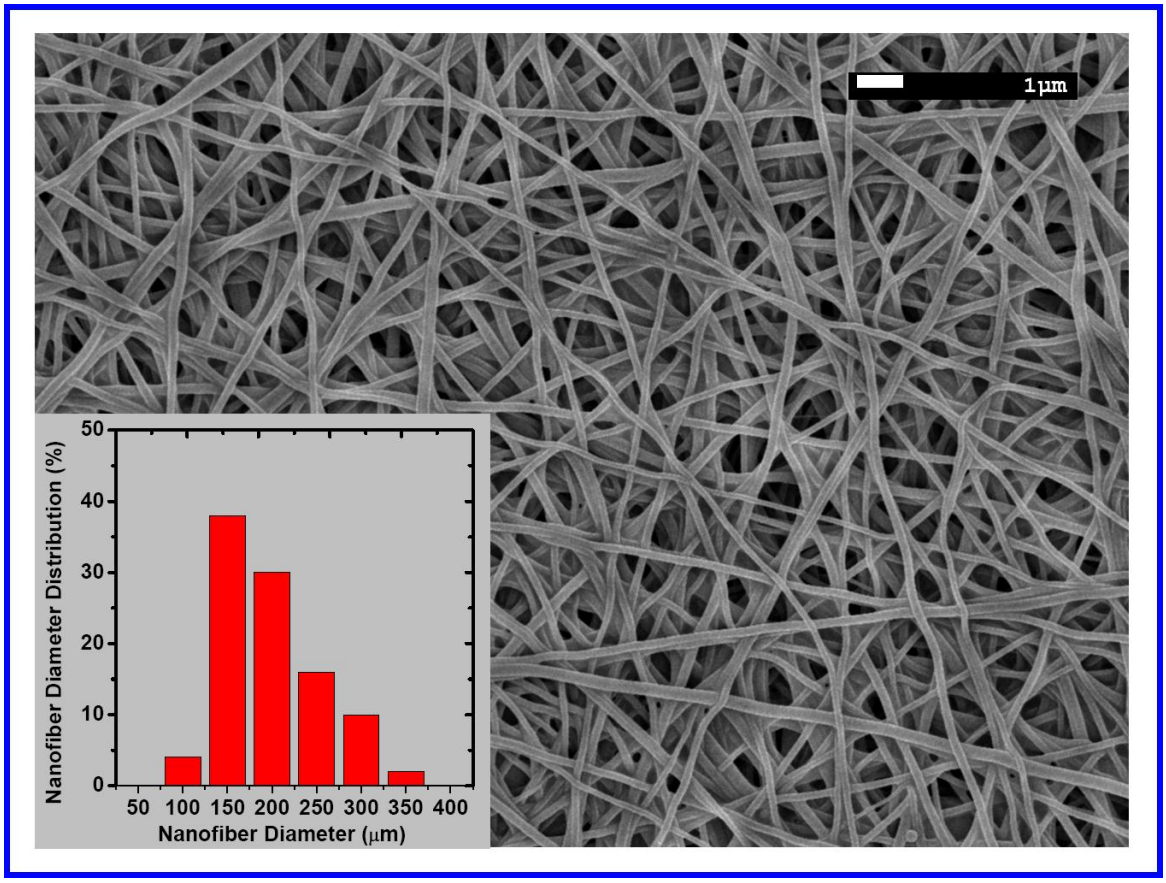

Figure S3. FESEM image of NSM top surface and its according nanofiber diameter distribution (inserted plot) with more than 70% nanofibers in the range of 100-200 nm and 98% nanofibers in the range of 100-300 nm.

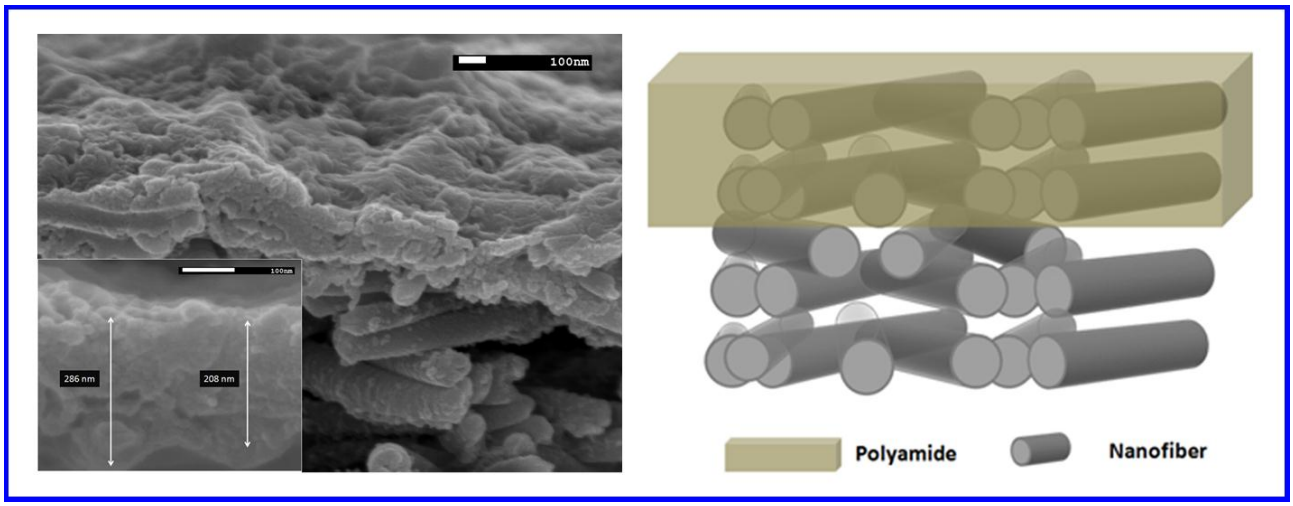

Figure S4. On the left is a typical FESEM high resolution image shows cross section of TNC-PRO membranes (top surface). The thickness of polyamide salt-rejecting layer is typically around 200-300 nm. On the right is a schematic model showing 1-2 layers of nanofiber becomes "backbones" of the surface polyamide selective layer.

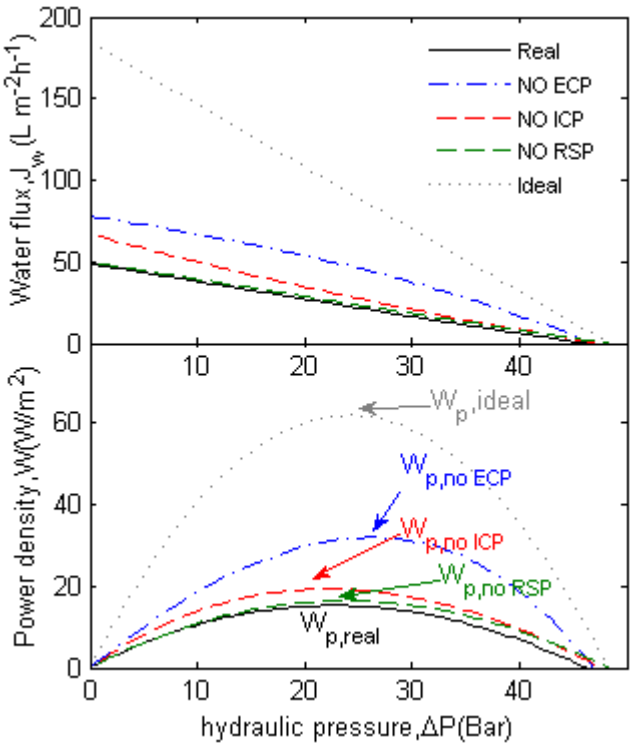

Figure S5. The J_W and W of TNC-2 PRO membranes as functions of ΔP. The lowest black curve shows real J_W and W considering all deleterious effects of ECP, ICP and RSP, while highest dotted grey curve shows hypothetical J_W and W assuming all deleterious phenomena are absent. In between, the dashed green, red and blue lines represent J_W and W assuming no RSP (i.e., B/J_W*[exp(J_WS/D)-exp(-J_W/k)]=0), ICP (i.e., exp(J_WS/D)=1) or ECP (i.e., exp(-J_W/k)=1) respectively.

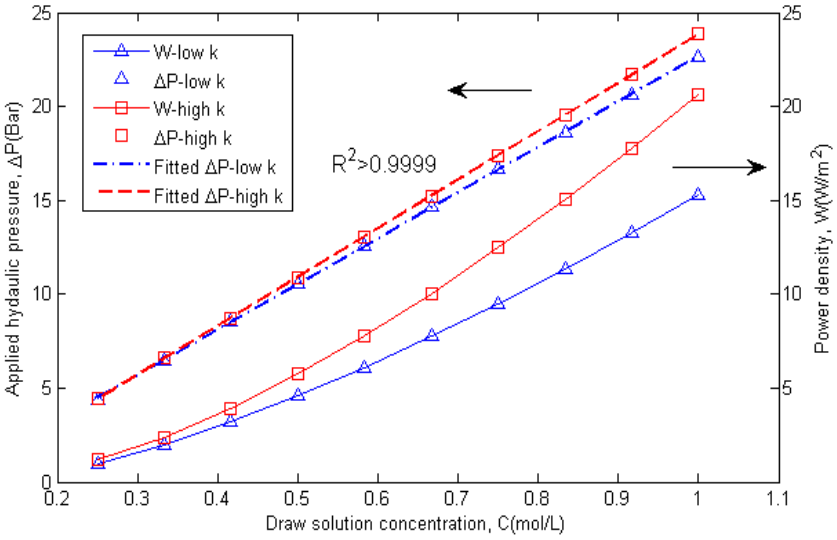

Figure S6. The relationships of optimum applied pressure ΔP and W_p with $C_{D,b}$. The optimum applied pressure is linearly decreased with the decrease of $C_{D,b}$. The red color and blue color represents a high k value of 180 L $m^{-2}h^{-1}$ and a low k value of 76.7 L $m^{-2}h^{-1}$, respectively.

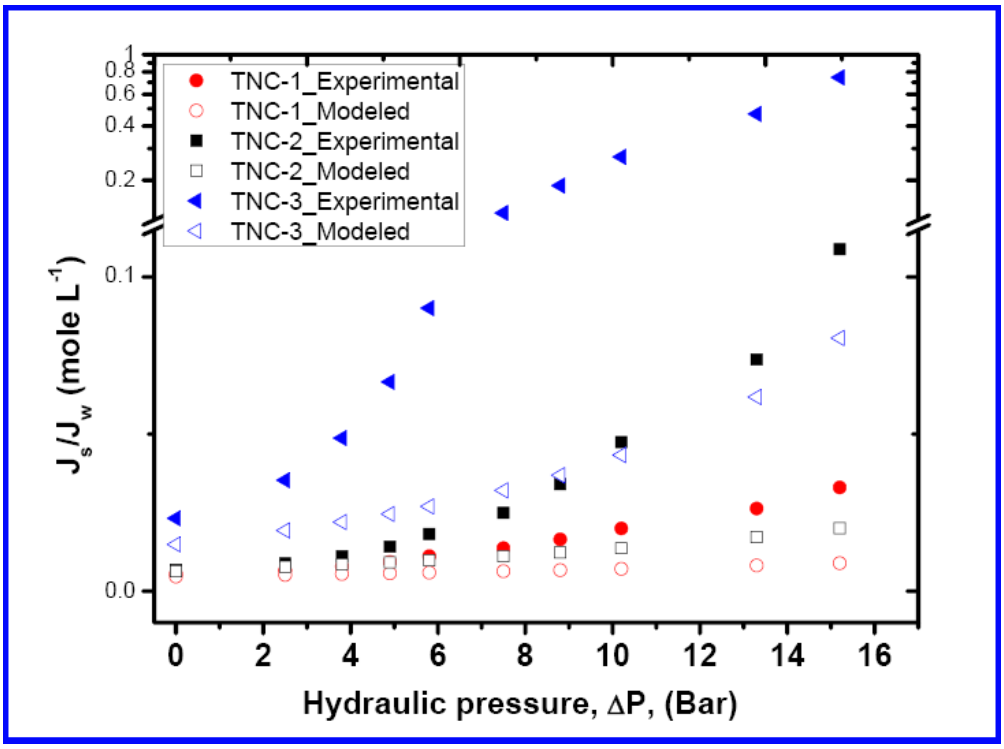

Figure S7. The specific reverse solute flux, J_S/J_W, versus the hydraulic pressure, ΔP.

Figure S8. The appearance comparison of TNC-PRO membrane before (left) and after (right) PRO operation.

References

1. Song, X.; Liu, Z.; Sun, D. D., Nano Gives the Answer: Breaking the Bottleneck of Internal Concentration Polarization with a Nanofiber Composite Forward Osmosis Membrane for a High Water Production Rate. *Advanced Materials* **2011,** *23*, (29), 3256-3260.

2. Yip, N. Y.; Tiraferri, A.; Phillip, W. A.; Schiffman, J. D.; Elimelech, M., High Performance Thin-Film Composite Forward Osmosis Membrane. *Environmental Science & Technology* **2010,** *44*, (10), 3812-3818.

3. Yip, N. Y.; Elimelech, M., Performance Limiting Effects in Power Generation from Salinity Gradients by Pressure Retarded Osmosis. *Environmental Science & Technology* **2011**.

4. Loeb, S.; Van Hessen, F.; Shahaf, D., Production of energy from concentrated brines by pressure-retarded osmosis : II. Experimental results and projected energy costs. *Journal of Membrane Science* **1976,** *1*, (1), 249-269.

5. Loeb, S.; Titelman, L.; Korngold, E.; Freiman, J., Effect of porous support fabric on osmosis through a Loeb-Sourirajan type asymmetric membrane. *Journal of Membrane Science* **1997,** *129*, (2), 243-249.